Journal of Energy Storage 69 (2023) 107936

Contents lists available at ScienceDirect

Journal of Energy Storage

journal homepage: www.elsevier.com/locate/est

Research Papers

Surface modification of jute fabrics by reduced graphene oxide-conducting polymer coatings for their application in low-cost and eco-friendly supercapacitors

J. Bonastre *, J. Molina, F. Cases

Departamento de Ingeniería Textil y Papelera, Escuela Politécnica Superior de Alcoy, Universitat Politècnica de València, Plaza Ferrándiz y Carbonell, s/n, 03801 Alcoy, Spain

ARTICLE INFO

Keywords:
Jute
Reduced graphene oxide
Polypyrrole
Eco-friendly
Supercapacitor

ABSTRACT

In this study, flexible textile supercapacitors were obtained on jute fabrics. Insulating jute fibers were converted into electrically conducting using an optimized reduced graphene oxide (rGO) deposition method. Supercapacitors were made of jute fabric and polypyrrole (PPy) as conducting polymer. rGO improved the electrical behavior of PPy-jute supercapacitors obtained by chemical polymerization. These chemical PPy-jute supercapacitors presented a low surface resistivity (6 Ω/sq) suitable for subsequent electrochemical polymerization. The best results were obtained for rGO-PPy-jute supercapacitors synthesized by electrochemical polymerization, with capacitance values of 5127 mF cm^{-2} (117 F g^{-1}) in a 3-electrode system; and1770 mF cm^{-2}, 39.9 F g^{-1}, 250 μW h cm^{-2} and 1100 μW cm^{-2} in a 2-electrode system. It is essential to highlight that the jute supercapacitors obtained are eco-friendly, low cost, flexible and with very competitive energy-storage values compared to recent investigations.

1. Introduction

Nowadays, the substitution of non-biodegradable materials (chemical derivatives of petroleum) with other biodegradable materials that respect the environment (eco-friendly) is unavoidable. More than 120.000 articles on eco-friendly topics and >245.000 about biodegradability issues show its importance and current interest [1]. A very interesting option is the use of natural fibers, which are renewable, biodegradable and non-toxic. From this point of view, many natural fibers can be used as: flax, hemp, bast, jute, coir, cotton and silk, among others. Their applications are numerous such as: building materials, automotive, biopolymers, packaging, medicine, etc. [2].

In this work, we consider advantageous to use jute as substrate to develop supercapacitors for the aforementioned reasons. In addition, the use of conducting polymers can be very suitable. Conducting polymers (CPs) [3–5] are advanced active materials in energy-storage systems such as supercapacitors. Polypyrrole (PPy) is a conducting polymer with pseudo-capacitive behavior, i.e., its high capacity is due to its high capacitance and faradaic processes due to the oxidation and reduction of its polymeric structure. In addition, PPy has thermochemical stability in a wide pH range [6–8]. Doping of PPy is needful to improve its electrical behavior. The size of the counter-ion is also essential for the electrical properties of PPy. The greater the size of the dopant, the lower proneness to be expelled from the polymeric structure, hence maintaining the electrical conductivity. The anthraquinone-2-sulfonic acid sodium salt was used as dopant due to its larger crystallite size [9].

Graphene could also improve the performance of conducting polymer supercapacitors on jute in this research work. Graphene is an outstanding material due to its high thermal and electron conductivity, physicochemical and mechanical properties, and large specific surface area, among others [10,11]. In addition, reduced graphene oxide (rGO) can enhance energy storage properties for conducting polymers presenting high capacitive behavior [12].

There are numerous studies on supercapacitors performed on flexible and foldable materials such as fibers and textile fabrics. Flexible materials are very advantageous for wearable energy storage devices. Many of them are combined with PPy, polyaniline, graphene, and carbon nanotubes, among others, such as:

- Polyaniline based supercapacitors:
  - Pani-graphene fiber shaped supercapacitor [13]
  - Pani-silk-multiwalled carbon nanotubes [14]

* Corresponding author.
E-mail address: joboca@txp.upv.es (J. Bonastre).

https://doi.org/10.1016/j.est.2023.107936
Received 24 March 2023; Received in revised form 15 May 2023; Accepted 3 June 2023
Available online 9 June 2023

- Nano-cellulose with polyaniline-graphene oxide-nanocarbon [15]
- Polypyrrole based supercapacitors:
  - MnO_2-cotton-carbon nanotubes deposited on PPy [16,17]
  - PPy-graphene oxide-polyacrylonitrile-nickel-plated-cotton [18]
- Other composite supercapacitors:
  - Transition metal phosphides on conductive fibers [19]
  - Nitrogen-boron-carbon nanotubes with activated carbon and cellulose fibers [20]
  - $NiCo_2S_4$-metallic cotton yarns [21]
  - MnO_2-carbonized cotton yarns [22]
  - Cotton-reduced graphene oxide-oxide silver nanoparticles [23]
  - Nickel-aluminium-cellulose-carbon nanotubes [24].

Jute has been used in this research because it is a very economical, biodegradable and eco-friendly material. The methods for synthesizing PPy on jute fabrics were also easy and did not require large amount of reagents or heat treatments at high temperatures. In this study, three different materials were synthesized directly on jute fabrics to obtain electrode materials for supercapacitors: chemically polymerized PPy on jute, chemically polymerized PPy on rGO-jute, and electrochemically synthesized PPy on rGO-jute. Insulating jute fibers were made electrically conducting by optimized deposition of rGO. Electrochemical characterization was performed by cyclic voltammetry (CV). The microscopic morphology of the different specimens was investigated using FESEM technique. The electrical properties were studied by electrochemical impedance spectroscopy (EIS). The values for energy storage were computed by galvanostatic charge-discharge (GCD) curves using 3 and 2-electrode system.

2. Experimental

2.1. Chemicals

Normapur acetone from VWR International Prolabo was used. Monolayer graphene oxide (GO) was acquired from Nanoinnova Technologies S.L. (Spain). Sodium dithionite ($Na_2S_2O_4$), sulfuric acid (H_2SO_4) and analytical grade pyrrole were acquired from Merck. Anthraquinone-2-sulfonic acid sodium salt (AQS) was purchased from Sigma-Aldrich. Elix 3 Millipore-Milli-Q Advantage A10 system provided ultrapure water to prepare the solutions. Oxygen was removed from the samples by bubbling nitrogen (N_2 premier X50S) when needed.

2.2. Jute fabric treatment

Common burlap fabric was provided by the company Hilaturas Ferre S.A. (Banyeres de Mariola-Spain). Jute fabrics have a surface density of 350 g/cm^2 and a density of 6 threads/cm. Jute fabric specimens were degreased with acetone in an ultrasonic bath for 30 min. Next, jute fabrics were cleaned with ultrapure water in an ultrasonic bath for 30 min. Finally, they were dried in an oven for 30 min at 80 °C [25].

2.3. Chemical synthesis of rGO

Firstly, 250 mL of 3 g L^{-1} graphene oxide (GO) solution was prepared sonicating GO powders in an ultrasonic bath for 30 min. The treated jute fabric, as Section 2.2, was immersed in the GO solution. GO adsorption elapsed for 30 min. The sample was then drawn from the solution and allowed to dry in ambient conditions for 24 h. The next stage was the reduction of GO to rGO. The dried GO-jute fabric was immersed in 0.05 M $Na_2S_2O_4$ solution at around 90 °C for 30 min [26]. Finally, the sample was washed with ultrapure water several times. In this way, the jute fabric coated with one rGO layer was obtained. This process was repeated several times to obtain samples with different number of rGO coatings, until the highest conductivity value for the specimens was reached.

2.4. Synthesis of PPy jute fabrics

Three different electrode materials were synthesized directly on jute fabrics to obtain electrode materials suitable for supercapacitors. Firstly, a chemical polymerization of PPy was carried out on the treated jute fabric (Section 2.2). Jute fabric was immersed in 200 mL of pyrrole + AQS solution for 30 min. Then 50 mL of $FeCl_3$ oxidizing reagent solution was added dropwise and polymerization continued during 15 h and finally the sample was extracted and washed with ultrapure water. The pyrrole concentration was 2 g L^{-1} and the molar ratios in the chemical synthesis were pyrrole:$FeCl_3$:AQS (1:2.5:0.6) [27]. This electrode material was named as PChem.

Chemical polymerization of PPy-AQS, as described above, was performed this time on rGO coated jute fabric (Section 2.3). This second electrode material was named as PRGOChem. The third electrode material was obtained by electrochemical polymerization of PPy-AQS in a three-electrode system with an Autolab PGSTAT302 potentiostat/galvanostat. PRGOChem was immersed in 0.20 M pyrrole + 0.03 M AQS solution. A conventional glass conical-shaped cell was used. The working electrode was a strip of PRGOChem with dimensions 1 × 3 cm. An area of 1 cm^2 was immersed into the synthesis solution. 2 stainless steel rods (4 mm diameter) were used as counter electrodes. An Ag/AgCl (3 M KCl) electrode was used as reference electrode. Electrochemical synthesis was carried out by potentiodynamic method. Eight cycles between 0.2 and 1.6 V and a scan rate of 5 mV s^{-1} were used [28]. This electrode material was named as PRGOElec.

To observe the different microscopic morphology characteristics of the samples obtained, a Zeiss Ultra 55 field emission scanning electron microscope (FESEM) from Oxford Instruments was used. An acceleration voltage of 1.5 kV was used and samples were not coated with a conductive coating.

2.5. Electrochemical measurements

Surface resistivity measurements of the specimens were carried out to optimize the number of rGO coatings to be applied on jute fabrics. The resistivity measurements were made with a surface resistivity meter, model SRM-232 from Guardian Manufacturing Inc. (0–2000 Ω/square), by the 4-point probe assembly. Cross-section conductivity measurements of specimens without electrolyte were also performed with an Autolab PGSTAT302 potentiostat/galvanostat using a two-electrode system (two copper discs 1.33 cm^2 was used). The impedance modulus in these samples was measured at a frequency of 0.01 Hz, and the amplitude of the sinusoidal voltage applied was ±5 mV.

PChem, PRGOChem and PRGOElec were characterized by EIS, CV and GCD curves (Autolab PGSTAT302 potentiostat/galvanostat). Firstly, 3-electrode system was used to control the potential of the working electrode. An ECC-Aqu from EL-CELL (Swagelok-type cell) test cell was used to characterize PPy jute fabrics. Working electrodes were PChem, PRGOChem and PRGOElec jute fabrics (5 × 5 mm and a mass of around 10 mg). Flexzorb™ FM10 activated carbon fabrics (from Chemviron Carbon) (5 × 5 mm) were used as counter electrodes. A gold tip was used as a pseudo-reference electrode (reference potential + 0.4 V vs Ag/AgCl (3 M Ag/AgCl) in 0.1 M H_2SO_4). Working and counter electrodes were arranged in sandwich configuration, separated by filter paper containing 0.1 M H_2SO_4. 2 gold discs of 18 mm diameter allowed electrical contact with the electrodes. Measurements were also made on identical specimens in a 2-electrode system. 2 similar samples (5 × 5 mm and mass around 10 mg) for each experiment were used as working and counter electrodes. The specific capacitance was calculated using the mass of the working electrode. For EIS studies, the experimental data were fitted with the proposed electrical equivalent circuits using a non-linear least squares fitting minimization method by ZView software. GCD curves for 3 days (100 cycles) were performed with an Interface 1010 Potentiostat/Galvanostat/ZRA equipment (Gamry Instruments, Inc.). The charge-discharge current density and voltage window were established from

Table 1
Surface resistivity and cross-section impedance measurements of jute, jute with 1 GO layer, and jute with several layers of rGO.

Specimens	Rs (Ω/sq)	|Z| a f = 0.01 Hz (Ω cm^2)
Jute	>2000	5,6·10^9
Jute-GO1	>2000	4,4·10^8
Jute-RGO1	1357	522
Jute-RGO2	605	209
Jute-RGO3	667	135
Jute-RGO4	621	136

CV.

3. Results and discussion

3.1. Coating of jute fabrics with rGO

rGO coatings were chemically synthesized on jute fabrics. GO adsorption and subsequent reduction with sodium dithionite were carried out as shown in Section 2.3. Table 1 shows the surface resistivity and cross-section impedance measurements of different specimens. Both jute and jute with one layer of GO (Jute-GO1) exhibited very high surface resistivity values. They overcame the maximum measurable with the surface resistivity meter (2000 Ω/sq). Similarly, the impedance modulus for cross-section measurements was very high, typical of non-electrically conducting materials. The cross-section measurements are very suitable since the configuration often used in supercapacitors is a sandwich arrangement, with the electric current flowing crosswise to the electrodes. When jute with one layer of GO was reduced with 0.05 M $Na_2S_2O_4$ (Jute-RGO1), a marked decrease in the surface resistivity value was demonstrated compared with the previous sample without reduction, Jute-GO1. Moreover, looking at the impedance module values, where the measurement range is higher, a significant decrease of almost six orders of magnitude was observed, comparing samples Jute-GO1 and Jute-RGO1. GO adsorption and reduction processes were performed two, three and four times. The surface resistivity and impedance modulus values seem to stabilize and reach the minimum (optimal) values for this type of jute fabric specimens. Fig. 1 shows FESEM micrographs for jute fabrics and jute fabrics covered by four rGO coatings. Comparing Fig. 1a and b, it can clearly be seen how the jute fabric is completely coated by rGO. The morphology displayed in Fig. 1b shows the typical wrinkled and kinked veil characteristic of graphene derivatives.

3.2. Electrochemical characterization of PPy/AQS jute fabrics. 3-electrode system

Three types of PPy/AQS synthesis were performed on jute samples:

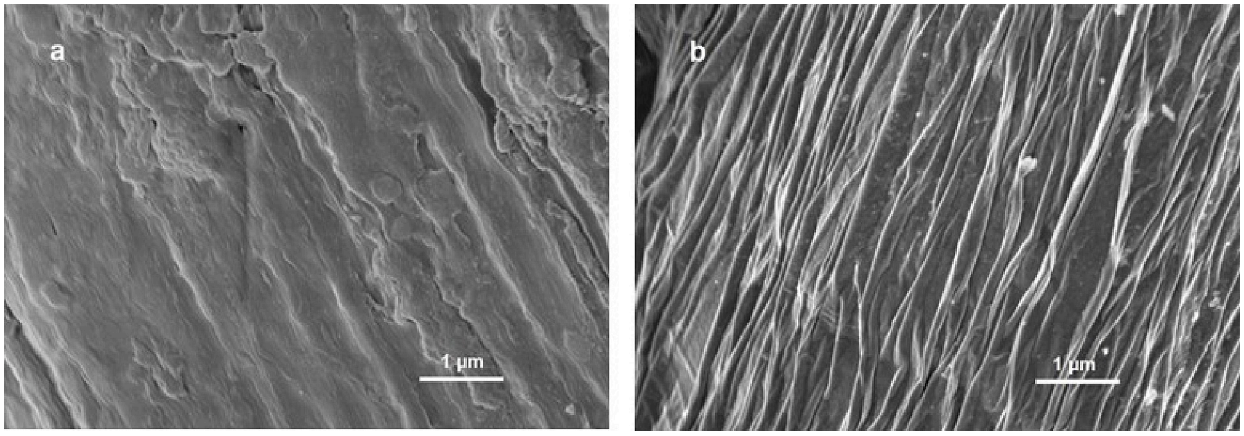

Fig. 1. (a) Micrograph for jute fabric and (b) micrograph for jute fabric covered by 4 coatings of rGO at 15 Kx.

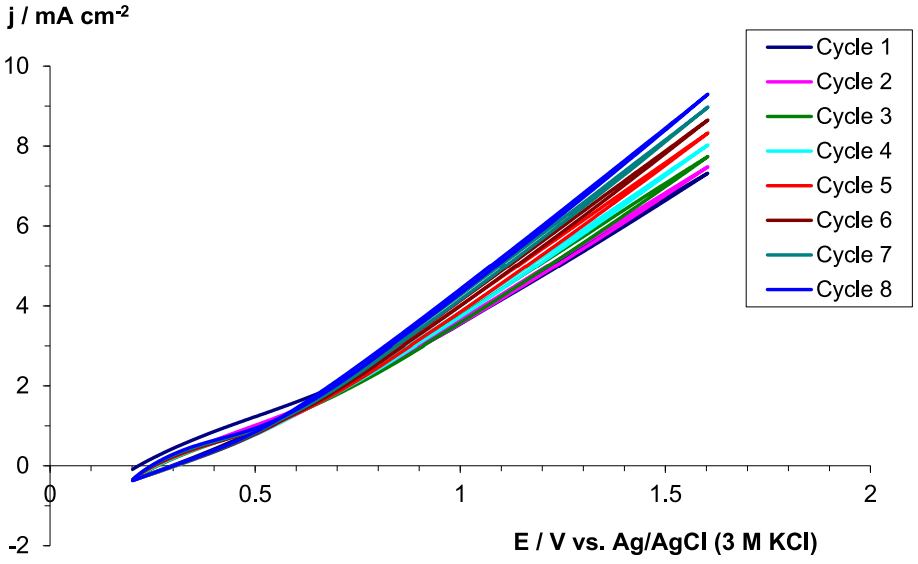

Fig. 2. CV curves for the synthesis in 0.20 M pyrrole + 0.03 M AQS on PRGOChem electrode at 5 mV s^{-1}. 1 cm^2 area.

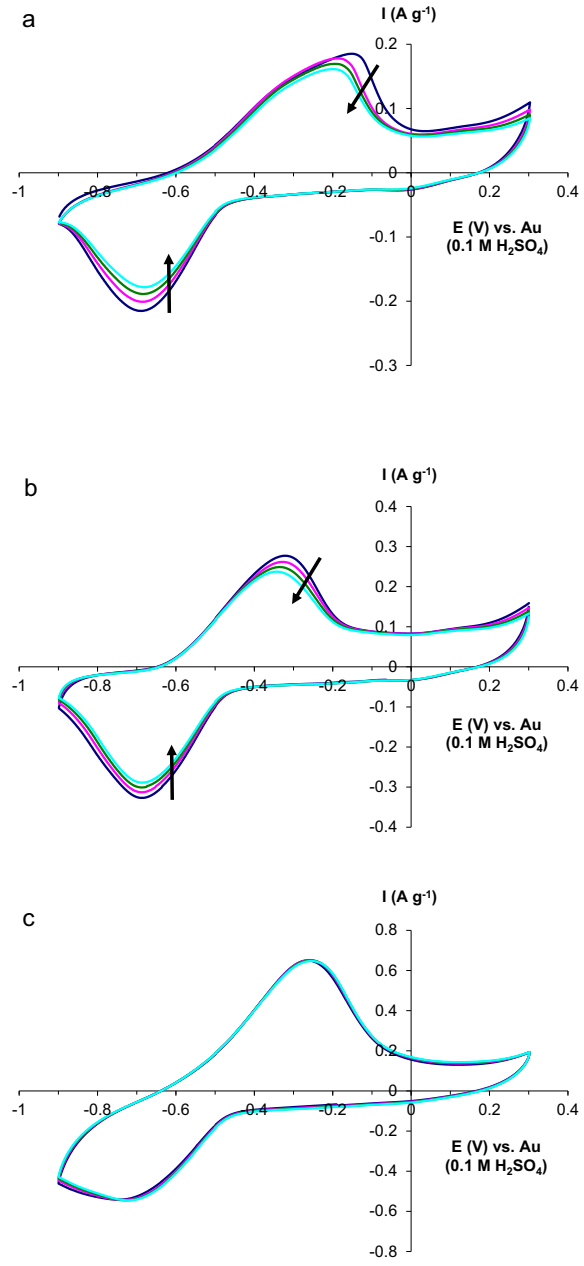

Fig. 3. First CV cycles recorded for the three-electrode system (Swagelok-type cell) in 0.1 M H_2SO_4 at a scan rate of 2.5 mV s^{-1}: (a) PChem, (b) PRGOChem and (c) PRGOElec.

chemical synthesis directly on jute fabrics (PChem), chemical synthesis on jute-RGO4 (PRGOChem) and electrochemical synthesis on PRGO-Chem (PRGOElec). The surface resistivity value for PRGOChem was 6 Ω/sq. This value was very low, which indicates a low ohmic drop for this material. For this reason, it was considered suitable to also carry out the electrochemical synthesis on that substrate. Methods were described in Section 2.4. The last two electrode materials were obtained on rGO-jute samples. In these specimens, four layers of rGO were deposited on jute, according to the optimized process aforementioned. Fig. 2 shows the CV curves obtained in the electrochemical PPy/AQS synthesis. It can be clearly seen how starting from 0.6 V, the current response increased with the number of cycles. At 1.6 V, the current intensity increased from around 7 mA in the first cycle to 9 mA in the eighth cycle (about a 30 % increase). This demonstrates the growth of polymer coating on the substrate.

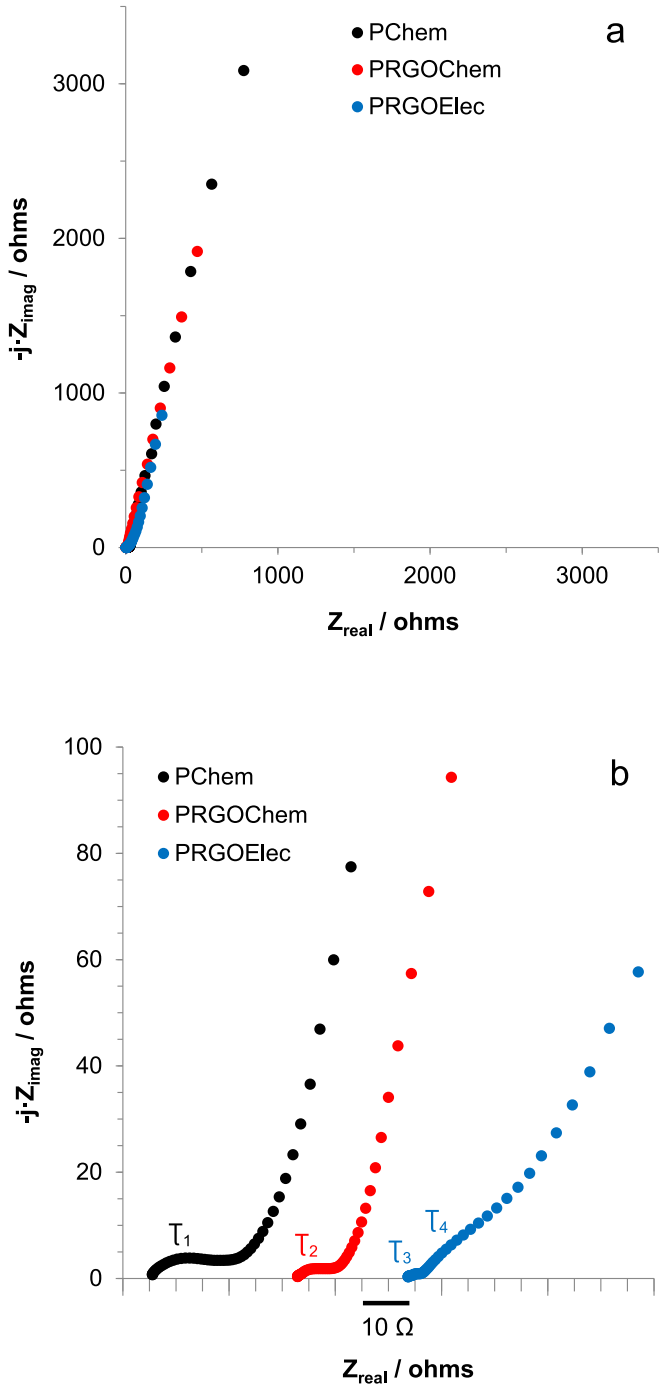

Fig. 4. Nyquist plots for the three-electrode system (Swagelok-type cell) in 0.1 M H_2SO_4 for: ● PChem, ● PRGOChem and ● PRGOElec. 0.25 cm^2 area. (a) Frequency range from 10^5 to 10^{-3} Hz. (b) Enlarged image of panel a.

The three electrode materials, PChem, PRGOChem and PRGOElec, were electrochemically characterized by CV. Fig. 3 shows the first voltammetric cycles for each sample immersed in 0.1 M sulfuric acid solution. Two peaks corresponding to the oxidation-reduction electrochemical process of the polymeric structure can be clearly seen in the voltammograms [29–31]. The CV curves for PRGOElec (Fig. 3c) confirm a much higher cycling stability than those for PChem (Fig. 3a) and PRGOChem (Fig. 3b) electrode materials. The first cycles for PRGOElec appear overlapping and practically cannot be distinguished. Also, the current density of the anodic and cathodic peaks decreases as the number of voltammetric cycle for PChem and PRGOChem increase.

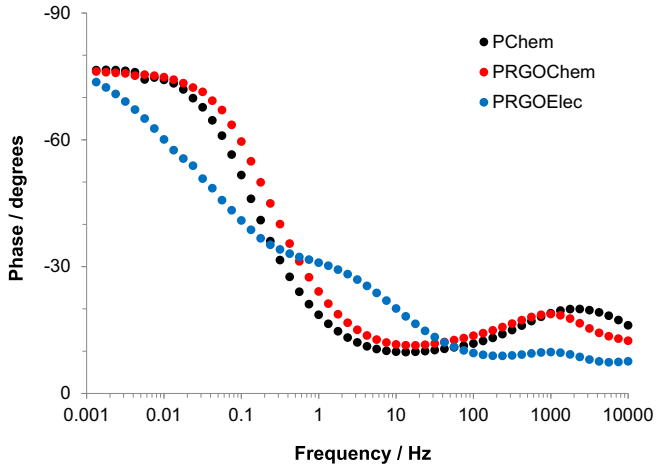

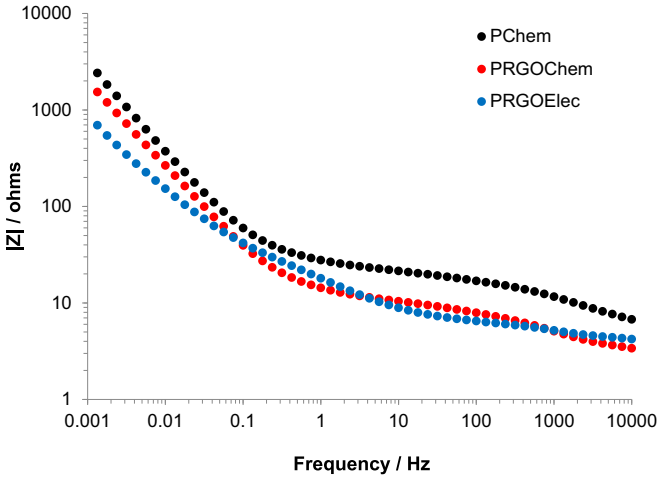

Fig. 5. Bode plots for the three-electrode system (Swagelok-type cell) in 0.1 M H_2SO_4 for: ● PChem, ● PRGOChem and ● PRGOElec. 0.25 cm^2 area. Frequency range from 10^5 to 10^{-3} Hz.

It is also important to note the increase in current density (increase around 50 %) for the oxidation and reduction peaks in PRGOChem (Fig. 3b) compared with PChem (Fig. 3a). It is evident how the incorporation of rGO into the coating improved the current density for anodic and cathodic peaks. Moreover, the current density increased even more for PRGOElec, around 300 %, compared with PChem electrode material. The incorporation of rGO and the electrochemical polymerization improved the electrochemical behavior of the analyzed specimens. It is expected that the characteristic charge storage parameters of the supercapacitor will also improve, as will be seen in later sections.

3.3. EIS study of PPy/AQS jute fabrics. 3-Electrode system

To obtain more information about the electrical response of the specimens, EIS analyses were performed on PChem, PRGOChem and PRGOElec samples. Fig. 4 shows Nyquist plots for the three specimens immersed in 0.1 M H_2SO_4. Typical pseudo-capacitive behavior can be observed for the three samples in Fig. 4a [32]. Fig. 4b displays a magnified image of Fig. 4a. A RC semicircle can be seen at high frequencies for PChem and PRGOChem samples (τ_1 and τ_2 time constants, respectively). Then, at low frequencies, the pseudo-capacitive behavior can be clearly seen in both samples. However, the PRGOElec specimen presents 2 time constants (τ_3 and τ_4) and the pseudo-capacitive behavior as shown in Fig. 4b. Looking at the phase angle vs frequency

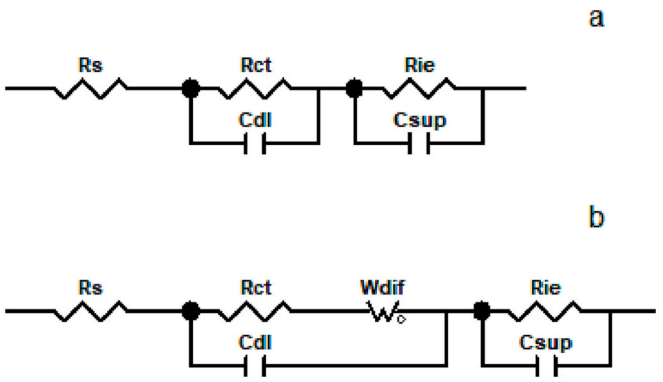

Fig. 6. Electrical equivalent circuit model used for: (a) PChem - PRGOChem and (b) PRGOElec.

Table 2
Results of impedance fitting data for: (a) PChem, (b) PRGOChem and (c) PRGOElec. 0.25 cm^2 area. Frequency range from 10^5 to 10^{-3} Hz.

Supercapacitors	PChem	PRGOChem	PRGOElec
Rs (Ω)	6.5	3.4	3,7
Rct (Ω)	16.0	7.7	1.2
Cdl (F)	$2.2{\cdot}10^{-5}$	$8.8{\cdot}10^{-5}$	$1.8{\cdot}10^{-5}$
Ws-R (Ω)	–	–	82.2
Ws-T (s)	–	–	10.4
Ws-P	–	–	0.44
Csup (F)	0.040 (4.9 F g^{-1})	0.054 (5.3 F g^{-1})	0.325 (29.6 F g^{-1})
Rie (Ω)	7396	4374	29

plot (Fig. 5), the relaxation processes for the specimens can be more clearly seen. PChem and PRGOChem show similar behavior at high and low frequencies. Nonetheless, one more relaxation process appears at middle frequencies (100–1 Hz) for the PRGOElec sample. The impedance modulus vs. frequency plot (Fig. 5) also shows how the impedance modulus at low frequencies for the PRGOElec sample presents the lowest value of all samples.

The experimental impedance data obtained allow us to propose 2 differentiated electrical equivalent circuits for the analyzed samples [32]. Fig. 6a shows the electrical equivalent circuit to model the electrical behavior of PChem and PRGOChem specimens. Fig. 6b shows the electrical equivalent circuit to model the impedance data for PRGOElec samples. In both electrical circuits, *Rs* corresponds to the electrolyte resistance. *Rct* is the charge transfer resistance and *Cdl* is the double layer capacitance at the interface associated in parallel with *Rct*. *Csup* is a capacitance regarding the high capacitance properties of the supercapacitors. *Rie* is the typical ion-ion charge transfer resistance for conducting polymers [33,34]. *Wdif* is the Warburg diffusion controlled by finite-length diffusion processes with reflective boundary conditions. *Ws*: diffusion of electroactive species in jute fabrics samples, *Ws-R*: diffusion resistance. *Ws-T*: l^2/D (s), *l*: length of the diffusion layer, *D*: diffusion coefficient. *Ws-P*: Warburg exponent [35].

The experimental data were fitted with the proposed electrical equivalent circuits using a non-linear least squares fitting minimization method by ZView software. Table 2 summarizes the impedance fitting data obtained. It can be seen how the *Rtc* decreases considerably from the PChem to the PRGOChem specimen, about half of its value. The incorporation of reduced graphene oxide improved the kinetics of the charge transfer process. In addition, the PRGOElec sample, which incorporates rGO and PPy conducting polymer coating, significantly diminishes *Rtc*, more than a tenfold decrease of the value for the PChem specimen. Looking at the voltammograms displayed in Fig. 3, the charge transfer resistance is clearly associated with the oxidation and reduction peaks of the polymeric structure of PPy/AQS. The PRGOElec specimen greatly improves the kinetics of the oxidation and reduction processes,

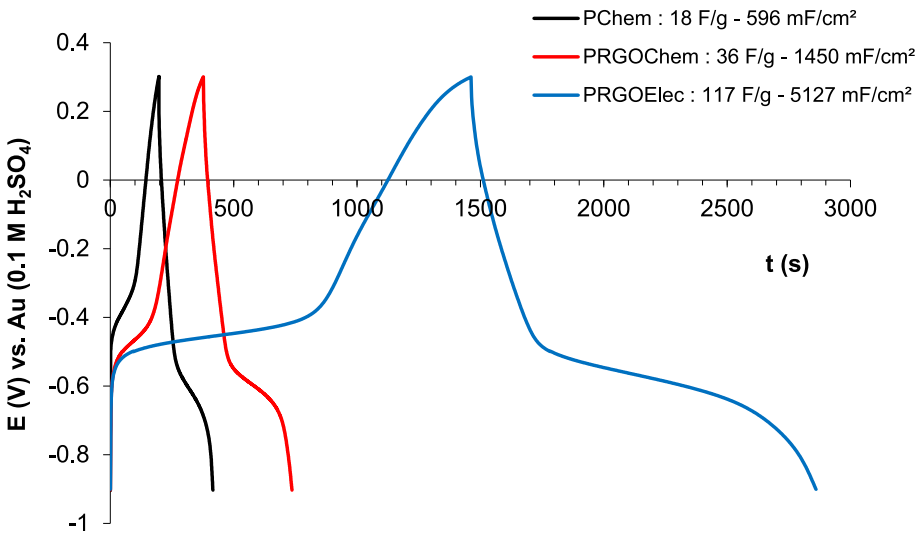

Fig. 7. GCD curves (4th cycle) for PChem, PRGOChem and PRGOElec samples obtained at a current density of 0.1 A/g.

due to the incorporation of rGO and the electrochemical synthesis of conducting polymer on the jute fabric. On the other hand, according to Table 2, a diffusional component appears for the PRGOElec sample. It must be note that this specimen presents rGO coatings, a chemically obtained PPy and a second PPy layer electrochemically deposited. That is why Warburg diffusion clearly appears for the PRGOElec specimen. However, this diffusional component did not prevent that PRGOElec sample had the best capacitance value, by far, as a supercapacitor (*Csup*) of those analyzed. The capacitance value for PRGOElec is about sixfold that of the PRGOChem specimen. The capacitance value for PRGOElec is around eightfold that of the PChem sample. The *Rie* presents a very marked decrease for the PRGOElec sample (29 Ω). This very low ion-ion charge transfer resistance value, to a great extent, makes possible the excellent behavior of the PRGOElec samples as high-performance supercapacitors.

3.4. Evaluation of the capacitance by GCD curves for PPy/AQS jute fabrics. 3-Electrode system

To obtain the specific capacitance in practical applications, GCD curves were obtained for PChem, PRGOChem and PRGOElec jute samples. A current density of 0.1 A/g was used to compare the electrical response of the different samples. Fig. 7 shows that all the samples present pseudo-capacitive behavior. Triangular zones with plateaus are typical of pseudo-capacitive materials, namely, the behavior of supercapacitors with faradaic reactions (conducting polymer oxidation/reduction). Fig. 7 shows how the PRGOChem sample improves the specific capacitance values (twofold) compared with the PChem specimen. rGO coating improved the specific capacitance values. A significant increase in the time scale can be easily seen for the PRGOElec sample. A high specific capacitance value of 117 F g^{-1} (6.5-fold higher than PChem) was obtained for PRGOElec. These values differ from those obtained by EIS. It is important to highlight that the values obtained by EIS in this study are representative of the capacitive process. Capacitance values obtained by GCD curves show the pseudo-capacitive components due to capacitive behavior (pure capacitor) and faradaic processes due to the oxidation and reduction of the PPy/AQS polymeric structure. Values obtained by GCD curves represent the overall capacity of the supercapacitor under study. On the other hand, it is important to note the capacitance values in relation to the area of the electrode materials. The areal capacitance also showed a high value for the PRGOElec sample. The values for PChem, PRGOChem and PRGOElec specimens were: 596 mF·cm^{-2}, 1450 mF·cm^{-2} and 5127 mF·cm^{-2}, respectively. rGO coatings and electrochemical synthesis markedly improved the specific and areal capacitance values for PPy/AQS jute fabrics. Besides, it is also important to stand out the high capacitance values obtained in materials that are economical and eco-friendly. Fig. 8 shows FESEM micrographs for PChem, PRGOChem and PRGOElec specimens.

PChem and PRGOChem show similar morphology at 5 Kx magnification (Fig. 8a and c). They present an abrupt and irregular morphology. The morphology significantly changes for the PRGOElec sample. An irregular filament-like structure with a globular structure can be seen in Fig. 8e. PChem and PRGOChem show also similar morphology at 15 Kx magnification (Fig. 8b and d). They have a rather irregular appearance, forming planes with different orientations, an abrupt morphology with valleys and sharp ridges. The morphology entirely changes for the PRGOElec sample. An irregular agglomerate of globular nature with spherical particles can be seen in Fig. 8f. This globular morphology is typical of PPy doped with large anions (AQS) and synthesized electrochemically on metal substrates [36]. The surface resistivity of PRGOChem was 6 Ω/sq, and therefore the morphology obtained for PRGOElec (deposited on PRGOChem) was similar to that obtained on metallic substrates. This morphology could increase the effective area of the PRGOElec sample, significantly improving the capacitance values which were determined by the GCD curves. Fig. 9 displays a fiber cross-section of PRGOElec sample. The typical globular morphology, as aforementioned, can also be seen in the cross-section micrograph.

3.5. Evaluation of specific capacitance and retention capacity for PPy/AQS jute fabrics. 2-Electrode system

For practical applications, in this section the electrical characterization was carried out in a 2-electrode cell system using the same sample (PChem, PRGOChem or PRGOElec) as working electrode and counter electrode. Fig. 10a shows the CV curves for PChem, PRGOChem and PRGOElec specimens at a scan rate of 2.5 mV s^{-1}. All CV curves practically showed capacitive behavior. A faradaic process can be slightly observed in the PRGOChem sample, probably due to processes of oxidation and reduction of PPy/AQS. The CV curves show a slightly higher capacity of the PRGOChem compared with PChem. Obviously, the PRGOElec specimen shows markedly higher capacitance than the previous samples. Fig. 10b shows the GCD curves for PChem, PRGOChem and PRGOElec specimens. As predicted by the voltammetric characterization, the specific capacitance (4th discharge curve shown) was higher for PRGOChem compared with PChem (10.6 and 12.1 F g^{-1}, respectively). Specific capacitance for PRGOElec was 3–4-fold higher (39.9 F g^{-1}) compared with the previous samples. Table 3 also shows capacitance (C_A), energy (E_A) and power (P_A) densities values. The

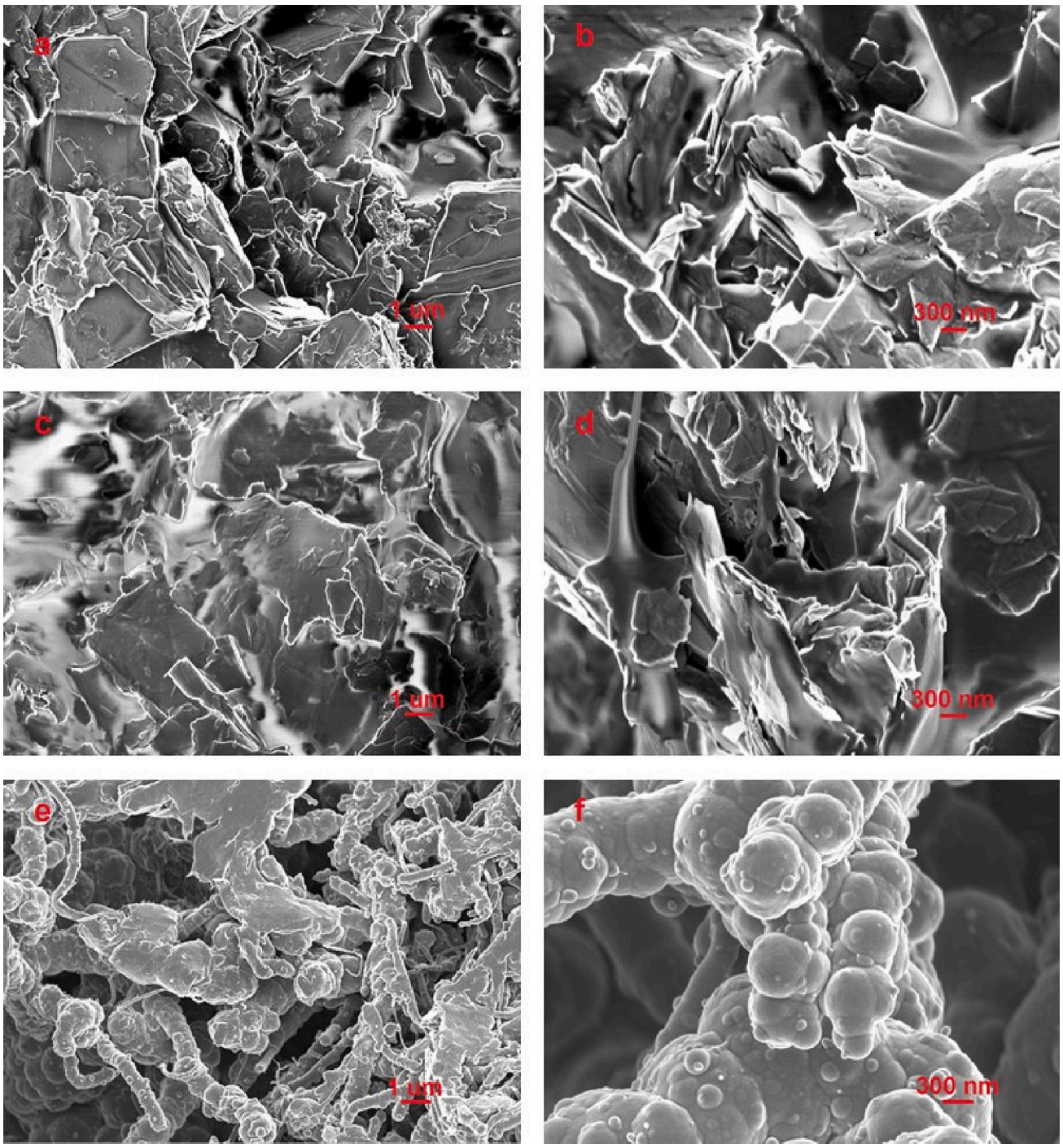

Fig. 8. FESEM micrographs for (a) PChem, (c) PRGOChem and (e) PRGOElec at 5 Kx, (b) PChem, (d) PRGOChem and (f) PRGOElec at 15 Kx.

energy density was calculated with the equation $E_A = C_A V^2/2$ where C_A is the areal capacitance (2-electrode system) and V is the voltage window. The power density was calculated as $P_A = E_A/t$ where E_A is the energy density and t the cell's discharge time. Areal capacitance showed marked differences between the samples. Areal capacitance for PRGOElec was also 3–4-fold higher than PChem and PRGOChem specimens. C_A, E_A and P_A values were significantly improved for PRGOChem compared to PChem. The incorporation of rGO into the PPy/AQS jute supercapacitor markedly improved the electrical behavior. The best values of C_A and E_A were obtained for the PRGOElec sample. A decrease in P_A was noted for the PRGOElec sample compared with the PRGOChem sample. As aforementioned in EIS section, a diffusion resistance (due to various coatings) of the electroactive species can explain this phenomenon. Therefore, a slightly slower electrical response (lower P_A) would be expected for the PRGOElec specimen. Anyway, all these parameters associated with the electrical properties of the PPy/AQS jute supercapacitors developed in this work, presented high and competitive values. Capacitance, energy and power density values (Ragone plots) for current devices, after consulting the most recent bibliography [37–39], were around [100–2000 mF cm^{-2}], [1–100 μW h cm^{-2}] and [10–2000 μW cm^{-2}], respectively. Table 3 show competitive values for PRGOElec (2-electrode system), 1770 mF cm^{-2}, 250 μW h cm^{-2} and 1100 μW cm^{-2}, for capacitance, energy and power density, respectively.

Finally, the evolution of the specific capacitance for PChem,

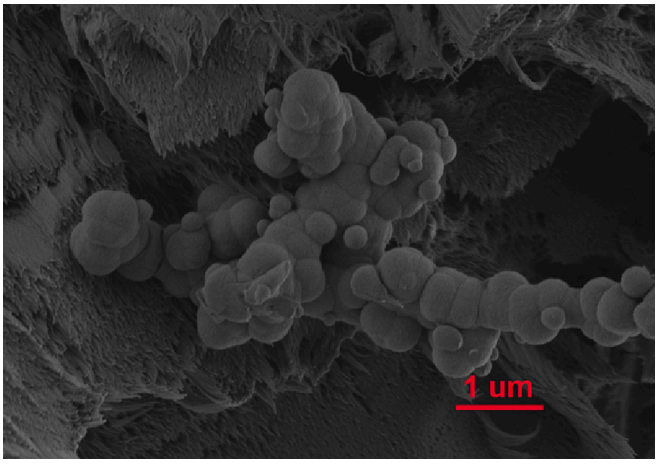

Fig. 9. FESEM cross-section micrograph for PRGOElec at 15Kx.

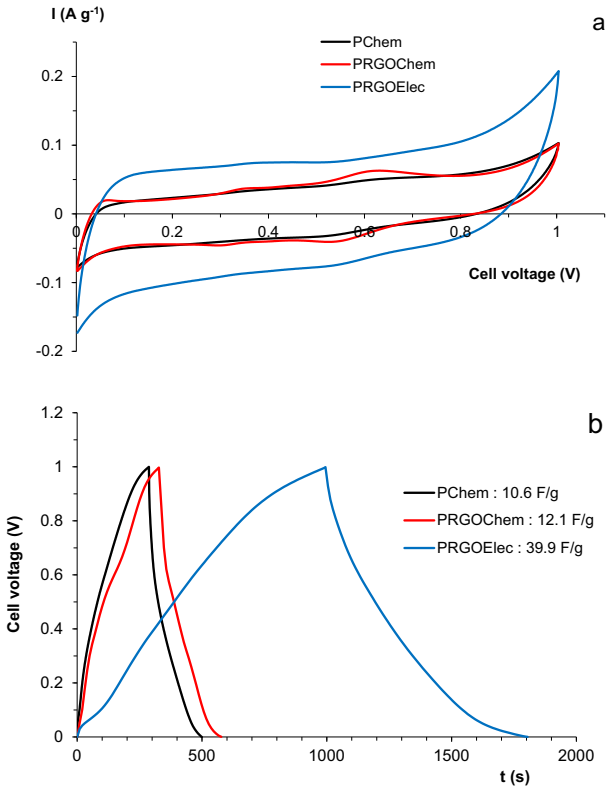

Fig. 10. (a) CV cycles recorded for PChem, PRGOChem and PRGOElec samples at a scan rate of 2.5 mV s^{-1}. (b) GCD curves (4th cycle) for PChem, PRGOChem and PRGOElec samples obtained at a current density of 0.05 A/g. Two-electrode system (Swagelok-type cell) in 0.1 M H_2SO_4.

Table 3
Areal values of capacitance (C_A), energy (E_A) and power densities (P_A) obtained with the two-electrode cell at 0.05 mA cm^{-2}.

Supercapacitors	C_A (mF cm^{-2})	E_A (μW h cm^{-2})	P_A (μW cm^{-2})
PChem	414	60	1000
PRGOChem	622	90	1300
PRGOElec	1770	250	1100

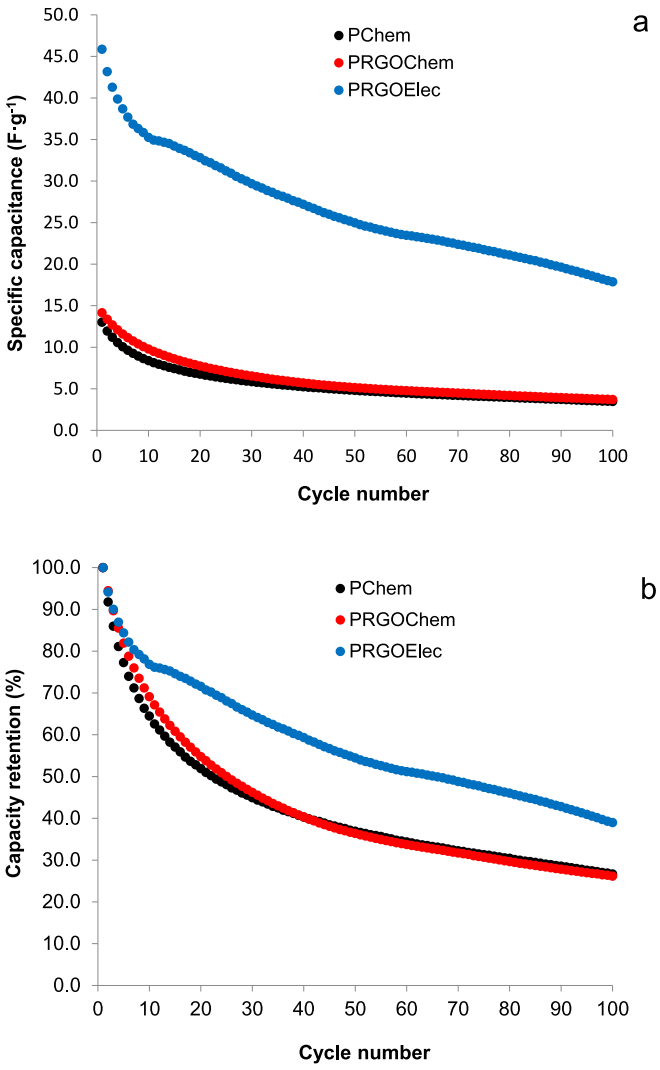

Fig. 11. Cycling stability tests for PChem, PRGOChem and PRGOElec at a current density of 0.05 A/g during 100 cycles: (a) Specific capacitance versus cycle number. (b) Capacity retention versus cycle number.

PRGOChem and PRGOElec specimens was recorded during 100 GCD cycles. Fig. 11a shows the specific capacitance vs cycle number plot. The specific capacitance is slightly higher for PRGOChem compared with the PChem sample. But above all, it is important to note how the highest specific capacitance value for the PRGOElec sample can be seen throughout the test. The capacitance is significantly higher for this specimen. Fig. 11b shows how also the capacity retention is significantly higher for PRGOElec compared with PChem and PRGOChem samples. Capacity retention is firstly also slightly higher for PRGOChem compared with PChem. However, the capacity retention values should be improved for all the PPy/AQS jute fabric samples. Therein, the adhesion of rGO and conducting polymer coatings on jute was insufficient to maintain the capacity with the number of charge-discharge cycles. Plasma treatment on jute + bovine serum albumin could improve the adhesion of PPy-jute supercapacitors [40]. Besides, a higher number of rGO coatings on jute fabric could improve the cycling stability, as it was achieved in a previous study on activated carbon cloth [28]. More work is in progress to improve these obtained values.

4. Conclusions

Insulating jute fabrics were converted into electrically conducting by rGO coatings. This allowed to carry out the electrochemical synthesis of

PPy on jute/rGO fabrics. rGO improved the electrical properties of PPy/AQS jute supercapacitors obtained by chemical polymerization. In addition, these chemically obtained PPy-rGO jute fabrics presented a low surface resistivity of 6 Ω/sq. This low surface resistivity allowed an improved subsequent electrochemical polymerization. The electrochemical synthesis of PPy/AQS on jute-rGO fabrics significantly increased the capacitance and specific energy values. The results for jute supercapacitors obtained by electrochemical polymerization were: 1770 mF cm^{-2} (39.9 F g^{-1}), 250 μW h cm^{-2} and 1100 μW cm^{-2} in 2-electrode system (and 5127 mF·cm^{-2} and 117 F g^{-1} in a 3-electrode system). These values are very competitive with the current flexible supercapacitors reviewed in the literature. It is very important to note the simplicity, low cost, biodegradability and eco-friendly of these PPy-rGO jute supercapacitors obtained in this work.

Declaration of competing interest

The authors declare that they have no known competing financial interests or personal relationships that could have appeared to influence the work reported in this paper.

Data availability

Data will be made available on request.

Acknowledgements

This research is part of the Spanish R + D + i contract PDC2021-121617-C22 funded by MCIN/AEI/10.13039/501100011033 and by the "European Union NextGenerationEU/PRTR" as well as the Red E3Tech Plus: Proyecto Redes de Investigación de la AEI Network E3Tech PLUS (RED2022-134552-T) project. Funding for open access charge: CRUE-Universitat Politècnica de València. Electron Microscopy Service of Universitat Politècnica de València is gratefully acknowledged for help with FESEM microscope.

References

[1] ScienceDirect®, Available on line: https://www.sciencedirect.com (accessed on March 13, 2023).
[2] Handbook of natural fibres, in: R.M. Kozlowski, M. Mackiewicz-Talarczyk (Eds.), Processing and Applications, Second edition vol. 2, The Textile Institute: Woodhead Publishing, Duxford, England; Cambridge, Massachusetts; Kidlington, England, 2020.
[3] Md.Y. Bhat, S.A. Hashmi, M. Khan, D. Choi, A. Qurashi, Frontiers and recent developments on supercapacitor's materials, design and applications: transport and power system applications, J. Energy Storage 58 (2023), 106104.
[4] S. Raza, X. Li, F. Soyekwo, D. Liao, Y. Xiang, C. Liu, A comprehensive overview of common conducting polymer-based nanocomposites; recent advances in design and applications, Eur. Polym. J. 160 (2021), 110773.
[5] H.W. Park, K.C. Roh, Recent advances in and perspectives on pseudocapacitive materials for supercapacitors-a review, J. Power Sources 557 (2023), 232558.
[6] Z. Li, Z. Lei, Y. Wang, Y. Wu, M. Guo, Y. He, J. Chen, J. Wang, A flexible and capsular polypyrrole nanotubular film-based pseudo-capacitive electrode with enhanced capacitive properties enabled by Au nanoparticle doping, J. Mater. Chem. C 8 (2020) 3807–3813.
[7] B.M. Hryniewicz, R.V. Lima, F. Wolfart, M. Vidotti, Influence of the pH on the electrochemical synthesis of polypyrrole nanotubes and the supercapacitive performance evaluation, Electrochim. Acta 293 (2019) 447–457.
[8] J. Yan, S. Sy, H. Wang, Y. Zhang, A.P. Yu, L.Z. Wang, L.M. Zhou, Synthesis of polypyrrole-coated NiO/$Ni(OH)_2$ hybrid flowers composite by pulse electropolymerization for supercapacitor with improved electrochemical capacitance, Int. J. Electrochem. Sci. 15 (2020) 12644–12653.
[9] A. Shukla, K. Sen, D. Das, Studies on electrolytic and doping behavior of different compounds and their combination on the electrical resistance of polypyrrole film via electrochemical polymerization, J. Appl. Polym. Sci. 139 (2022), e52793.
[10] A.K. Geim, K.S. Novoselov, The rise of graphene, Nat. Mater. 6 (2007) 183–191.
[11] V.B. Mbayachi, E. Ndayiragije, T. Sammani, S. Taj, E.R. Mbuta, A.U. Khan, Graphene synthesis, characterization and its applications: a review, Results Chem. 3 (2021), 100163.
[12] A. Razaq, F. Bibi, X. Zheng, R. Papadakis, S.H.M. Jafri, H. Li, Review on graphene-, graphene oxide-, reduced graphene oxide-based flexible composites: from fabrication to applications, Materials 15 (2022) 1012.
[13] X. Zheng, L. Yao, Y. Qiu, S. Wang, K. Zhang, Core–sheath porous polyaniline nanorods/graphene fiber-shaped supercapacitors with high specific capacitance and rate capability, ACS Appl. Energy Mater. 2 (2019) 4335–4344.
[14] P. Song, J. Tao, X. He, Y. Sun, X. Shen, L. Zhai, A. Yuan, D. Zhang, Z. Ji, B. Li, Silk-inspired stretchable fiber-shaped supercapacitors with ultrahigh volumetric capacitance and energy density for wearable electronics, Chem. Eng. J. 386 (2020), 124024.
[15] S. Lyu, Y. Chen, L. Zhang, S. Han, Y. Lu, Y. Chen, N. Yang, Z. Chena, S. Wang, Nanocellulose supported hierarchical structured polyaniline/nanocarbon nanocomposite electrode via layer-by-layer assembly for green flexible supercapacitors, RSC Adv. 9 (2019) 17824–17834.
[16] G. Cai, B. Hao, L. Luo, Z. Deng, R. Zhang, J. Ran, X. Tang, D. Cheng, S. Bi, X. Wang, K. Dai, Highly stretchable sheath–core yarns for multifunctional wearable electronics, ACS Appl. Mater. Interfaces 12 (2020) 29717–29727.
[17] B. Hao, Z. Deng, S. Bi, J. Ran, D. Cheng, L. Luo, G. Cai, X. Wang, X. Tang, In situ polymerization of pyrrole on CNT/cotton multifunctional composite yarn for supercapacitors, Ionics 27 (2021) 279–288.
[18] X. Zhao, W. Li, F. Li, Y. Hou, T. Lu, Y. Pan, J. Li, Y. Xu, J. He, Wearable yarn supercapacitors coated with twisted PPy@GO nanosheets and PPy@PAN-GO nanofibers, J. Mater. Sci. 56 (2021) 18147–18161.
[19] L. Xie, Q. Zong, Q. Zhang, J. Sun, Z. Zhou, B. He, Z. Zhu, S. E, Y. Yao, Hierarchical NiCoP nanosheet arrays with enhanced electrochemical properties for high-performance wearable hybrid capacitors, J. Alloys Compd. 781 (2019) 783–789.
[20] H. Hu, X. Sun, W. Chen, J. Wang, X. Li, Y. Huang, C. Wei, G. Liang, Electrochemical properties of supercapacitors using boron nitrogen double-doped carbon nanotubes as conductive additive, Nano 14 (07) (2019) 1950080.
[21] Y.-F. Wang, H.-T. Wang, S.-Y. Yang, Y. Yue, S.-W. Bian, Hierarchical NiCo2S4@nickel–cobalt layered double hydroxide nanotube arrays on metallic cotton yarns for flexible supercapacitors, ACS Appl. Mater. Interfaces 11 (2019) 30384–30390.
[22] S. Ullah, J. Yu, H. Liu, W. Iqbal, B. Yang, C. Li, C. Zhu, J. Xu, Fabrication of MnO2-carbonized cotton yarn derived hierarchical porous active carbon flexible supercapacitor electrodes for potential applications in cable-type devices, Appl. Surf. Sci. 487 (2019) 180–188.
[23] W. Xiao, J. Huang, W. Zhou, Q. Jiang, Y. Deng, Y. Zhang, L. Tian, Surface modification of commercial cotton yarn as electrode for construction of flexible fiber-shaped supercapacitor, Coatings 11 (2021) 1086.
[24] S. Acharya, S. De, G.C. Nayak, CNT/LDH-stabilized biomass-derived nanocellulose as a low-cost alternative for asymmetric supercapacitors: impact of sources of nanocellulose, ACS Appl. Electron. Mater. 5 (2023) 406–417.
[25] L. Manjakkal, F. Fantinelli Franco, A. Pullanchiyodan, M. González-Jiménez, R. Dahiya, Natural jute fibre-based supercapacitors and sensors for eco-friendly energy autonomous systems, Adv. Sustain. Syst. 5 (2021) 2000286.
[26] B. Fugetsu, E. Sano, H. Yu, K. Mori, T. Tanaka, Graphene oxide as dyestuffs for the creation of electrically conductive fabrics, Carbon 48 (2010) 3340–3345.
[27] J. Molina, A.I. del Río, J. Bonastre, F. Cases, Chemical and electrochemical polymerisation of pyrrole on polyester textiles in presence of phosphotungstic acid, Eur. Polym. J. 44 (2008) 2087–2098.
[28] J. Fernández, J. Bonastre, J. Molina, F. Cases, Electrochemical study on an activated carbon cloth modified by cyclic voltammetry with polypyrrole/anthraquinone sulfonate and reduced graphene oxide as electrode for energy storage, Eur. Polym. J. 103 (2018) 179–186.
[29] S. Konwer, R. Boruah, S.K. Dolui, Studies on conducting polypyrrole/graphene oxide composites as supercapacitor electrode, J. Electron. Mater. 40 (11) (2011) 2248–2255.
[30] Ch. Zhu, J. Zhai, D. Wen, S. Dong, Graphene oxide/polypyrrole nanocomposites: one-step electrochemical doping, coating and synergistic effect for energy storage, J. Mater. Chem. 22 (2012) 6300–6306.
[31] Y. Yang, K. He, P. Yana, D. Wanga, X. Wua, X. Zhao, Z. Huang, Ch. Zhanga, D. Hea, Enhanced capacity of polypyrrole/anthraquinone sulfonate/graphene composite as cathode in lithium batteries, Electrochim. Acta 138 (2014) 481–485.
[32] J. Arjomandi, J.Y. Lee, F. Ahmadi, M.H. Parvin, H. Moghanni-Bavil-Olyaei, Spectroelectrochemistry and electrosynthesis of polypyrrole supercapacitor electrodes based on gamma aluminum oxide and gamma iron (III) oxide nanocomposites, Electrochim. Acta 251 (2017) 212–222.
[33] A. Lasia, B.E. Conway, J.O.M. Bockris, in: R.E. White (Ed.), Modern Aspects of Electrochemistry vol. 32, Kluwer Academic/Plenum Publishers, New York, 1999, p. 143.
[34] J.R. Macdonald, W.B. Johnson, in: J.R. Macdonald (Ed.), Impedance Spectroscopy: Emphasizing Solid Materials and Systems, Wiley, New York, 1987, p. 1.
[35] ZView® software from Scribner Associates Inc., 150 East Connecticut Avenue Southern Pines, North Carolina, USA 28387.
[36] K.W. Oh, H.J. Park, S.H. Kim, Electrical property and stability of electrochemically synthesized polypyrrole films, J. Appl. Polym. Sci. 91 (2004) 3659–3666.
[37] T. Guan, L. Shen, N. Bao, Hydrophilicity improvement of graphene fibers for high-performance flexible supercapacitor, Ind. Eng. Chem. Res. 58 (2019) 17338–17345.
[38] N. He, J. Liao, F. Zhao, W. Gao, Dual-core supercapacitor yarns: an enhanced performance consistency and linear power density, ACS Appl. Mater. Interfaces 12 (2020) 15211–15219.
[39] Y. Liang, X. Luo, Z. Hua, L. Yang, Y. Zhang, L. Zhu, M. Zhu, Deposition of ZIF-67 and polypyrrole on current collector knitted from carbon nanotube-wrapped polymer yarns as a high-performance electrode for flexible supercapacitors, J. Colloid Interface Sci. 631 (2023) 77–85.
[40] J. Molina, J. Fernández, M. Fernandes, A.P. Souto, M.F. Esteves, J. Bonastre, F. Cases, Plasma treatment of polyester fabrics to increase the adhesion of reduced graphene oxide, Synth. Met. 202 (2015) 110–122.